NANO LETTERS

pubs.acs.org/NanoLett Letter

Synthesis of Atomically Thin Hexagonal Diamond with Compression

Feng Ke,* Lingkong Zhang, Yabin Chen, Ketao Yin, Chenxu Wang, Yan-Kai Tzeng, Yu Lin, Hongliang Dong, Zhenxian Liu, John S. Tse, Wendy L. Mao, Junqiao Wu, and Bin Chen*

Cite This: *Nano Lett.* 2020, 20, 5916−5921 Read Online

ACCESS | Metrics & More | Article Recommendations | Supporting Information

ABSTRACT: Atomically thin diamond, also called diamane, is a two-dimensional carbon allotrope and has attracted considerable scientific interest because of its potential physical properties. However, the successful synthesis of a pristine diamane has up until now not been achieved. We demonstrate the realization of a pristine diamane through diamondization of mechanically exfoliated few-layer graphene via compression. Resistance, optical absorption, and X-ray diffraction measurements reveal that hexagonal diamane (h-diamane) with a bandgap of 2.8 ± 0.3 eV forms by compressing trilayer and thicker graphene to above 20 GPa at room temperature and can be preserved upon decompression to ∼1.0 GPa. Theoretical calculations indicate that a (−2110)-oriented h-diamane is energetically stable and has a lower enthalpy than its few-layer graphene precursor above the transition pressure. Compared to gapless graphene, semiconducting h-diamane offers exciting possibilities for carbon-based electronic devices.

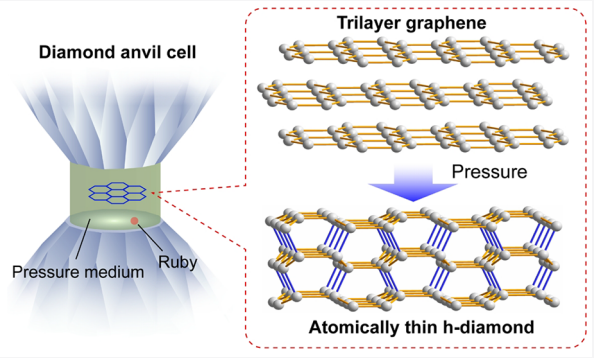

KEYWORDS: *Atomically thin diamond, Few-layer graphene, Bandgap, Electrical transport, Pressure*

Although diamond and graphite are both allotropes of carbon, their very different structures and bonding lead to dramatically different physical, chemical, and mechanical properties. Diamond is the hardest known bulk material, the best thermal conductor, chemically inert, and optically transparent compared to graphite, which is a soft, opaque semimetal. Atomically thin graphite, that is, graphene, has been found to have many exceptional physical properties, such as high carrier mobility,[1] half-integer quantum Hall effect,[2−4] and unconventional superconductivity.[5] An atomically thin diamond, that is, diamane is predicted to have dramatically different properties from graphene. Diamane has cubic (c-) and hexagonal (h-) polymorphs, analogous to c- and h-diamond. Each diamane polymorph possesses several predicted orientations, such as (100) and (111) orientations of c-diamane, and (0001) and (−2110) orientations of h-diamane,[6−8] depending on the crystallographic orientations from which c- or h-diamond is thinned down to the atomic thickness.

Synthesis of atomically thin diamond film and other group IV graphene analogues have attracted considerable theoretical and experimental efforts.[9] Previous studies suggest that atomically thin diamond films are not achievable in a pristine state because diamond processes a three-dimensional crystalline structure and would lack chemical stability when thinned down to the thickness of diamond's unit cell due to the dangling sp^3 bonds. Chemical functionalization of the surface carbons with specific chemical groups was considered necessary to stabilize the two-dimensional structure.[6−8,10−16] Surface hydrogenation or fluorination for synthesizing such diamond films, called diamane,[7,8,10] diamondol,[11] diamondene,[12] or diamene[13] have been attempted, and various substrates such as Co, Ni, Cu and SiC have also been used in these attempts.[13,17] The type of substrate has been found to impact the physical properties of graphene and diamond film significantly.[18−20] A diamondlike film was observed when a two-layer (buffer layer plus one layer) graphene was micro-indented, where the surface carbon atoms interacted strongly with the Si of SiC substrate.[13] The conversion was not observed in thicker (3- and 5-layer) graphene. A fluorinated c-diamane film has also recently been synthesized by chemical vapor deposition method.[10] Importantly, all of these attempts change the composition of materials.

Despite the significant experimental and theoretical efforts that have been invested, a pristine diamane has still not been achieved. Here, we used an alternative approach, diamondization of mechanically exfoliated few-layer graphene via compression, to synthesize the long sought after diamane film. The diamondization process is usually accompanied by an opening of an energy gap and a dramatic resistance increase

Received: April 29, 2020
Revised: June 23, 2020
Published: June 24, 2020

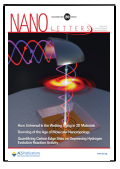

https://dx.doi.org/10.1021/acs.nanolett.0c01872
Nano Lett. 2020, 20, 5916−5921

due to the sp^2-sp^3 rehybridization between carbon atoms. Therefore, we studied the diamondization of mechanically exfoliated few-layer graphene by monitoring its electronic structure using electrical transport and optical absorption measurements. Our studies demonstrate that pristine h-diamane could be synthesized by compressing trilayer and thicker graphene to above 20 GPa, which once synthesized could be preserved to ~1.0 GPa upon decompression.

Using our recently developed photolithography-based microwiring technique to prepare film electrodes on a diamond surface for resistance measurements (Figure 1a), we studied the pressure-induced sp^2-sp^3 diamondization transition of mechanically exfoliated graphene (Figure S1) with layer thickness ranging from 12- to bilayer at room temperature. All of the samples except bilayer graphene show a dramatic resistance increase above the transition pressure (Figure 1b). The transition pressure depends greatly on the layer number, that is, the transition occurs at higher pressures in thinner samples. Specifically, the sheet resistance of 12-layer graphene varies smoothly until the onset of the transition just above 19.6 GPa followed by a substantial resistance increase of more than 3 orders of magnitude upon further compression to 50.0 GPa. Beyond this, the resistance value exceeds the measurable range of our instruments. Hexa-, tetra- and trilayer graphene show the same transition with the onset pressure shifting to ~21.3, ~27.1, and ~33.0 GPa, respectively. For bilayer graphene, however, the sheet resistance remains nearly constant with compression up to 60 GPa, the highest pressure studied in our measurements. The different behavior between bilayer and thicker (tri-, tetra-, hexa-, 12- and multilayer) graphene suggests that the pressure-induced transition is intrinsic to few-layer graphene and not caused by any interaction with the pressure medium we loaded (Daphne 7373 or Ar gas) or the carbon atoms of the diamond surface.

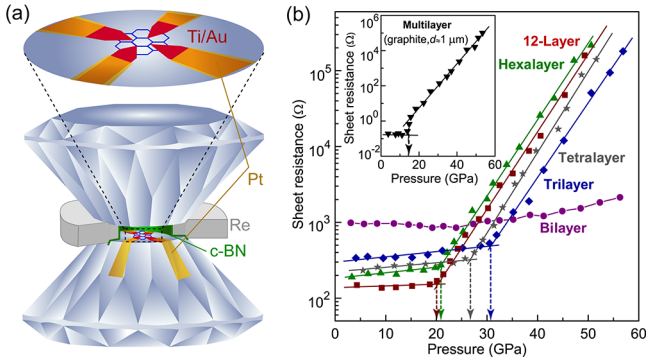

Figure 1. Sheet resistance of mechanically exfoliated 12-, hexa-, tetra-, and bilayer graphene as a function of pressure. (a) Cross-sectional schematic of the designed four-terminal nanodevices. Ti/Au film electrodes were patterned onto the diamond culet and extended with platinum foils. (b) Sheet resistance vs pressure curves for 12-, hexa-, tetra-, tri-, and bilayer graphene measured at room temperature. The solid lines are a guide for the eyes. The pressure dependence of the resistance of graphite is also done as a reference for comparison (inset).

As a comparison, we also studied the resistance evolution of graphite (1 μm in thickness) as a function of pressure. The resistance of graphite has the same behavior with those of 12-, hexa-, tetra-, and trilayer graphene (Figure 1b, inset), except for the resistance difference and slight shift of the transition pressure to ~15.1 GPa. The transition pressure is consistent with those observed in previous electrical results on the graphite to h-diamond transition under pressure[21,22] and other measurements.[23−30] The consistency of the pressure response suggests that the dramatic resistance increases in 12-, hexa-, tetra-, and trilayer graphene are caused by the pressure-induced sp^2-to-sp^3 diamondization transition. Higher pressures would be needed to induce the diamondization process in bilayer graphene if it were to occur. The pressure response of bilayer graphene is different from that of the double-layer graphene using water as the pressure medium.[12] The difference could be caused by the pressure medium. The double-layer graphene, studied in ref 12, transformed to diamondene with the surface carbons interacting with the hydrogen atoms of water/ice, while such an interaction was not observed in our studied few-layer graphene using Daphne 7373 or Ar gas as the pressure medium.

The resistance−temperature ($R-T$) curves of mechanically exfoliated graphene with layer thickness ranging from 12- to bilayer confirm the layer dependence of the sp^2-to-sp^3 diamondization transition (Figure S3). For all of the graphene

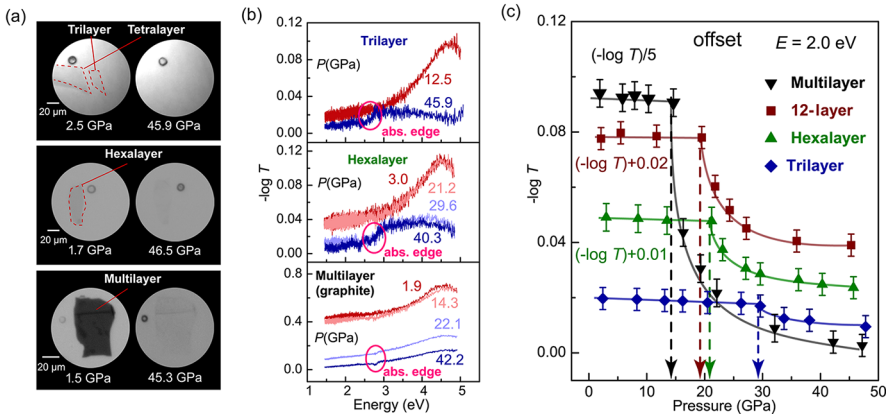

Figure 2. High-pressure optical absorption results of mechanically exfoliated tri-, hexa-, 12-, and multilayer graphene. (a) Optical microscopy images of compressed tri-, tetra-, hexa-, and multilayer graphene (graphite) samples in transmission mode with a white light source. (b) Optical absorbance of tri-, hexa-, and multilayer graphene as a function of pressure. The absorbance of the diamond and pressure medium has been subtracted. (c) Pressure dependence of the absorbance of tri-, hexa-, 12-, and multilayer graphene at a photon energy of 2.0 eV. The solid lines are a guide for the eyes.

https://dx.doi.org/10.1021/acs.nanolett.0c01872
Nano Lett. 2020, 20, 5916−5921

samples from 12-layer to trilayer, their resistances show weak positive temperature dependence ($dR/dT \approx 0$) before the transition. After the transition, for example, in trilayer graphene above 35.2 GPa, the temperature dependence of resistance becomes negative ($dR/dT < 0$) and increasingly steep during further compression, signaling a semiconducting behavior. However, in bilayer graphene the $R-T$ curve always shows weak temperature dependence up to 60 GPa. Graphite shows similar behaviors with 12-, hexa-, tetra-, and trilayer graphene.

The infrared (0.2−1.0 eV) and visible−ultraviolet (1.4−4.9 eV) absorption spectra further confirm the pressure-induced sp^2-sp^3 diamondization in mechanically exfoliated trilayer and thicker graphene. The absorbance of all the samples from tri- to 12-layer graphene shows an obvious transition above the onset pressure. Before the transition, a pronounced and asymmetric peak at a photon energy of 4.6 eV is observed in the absorption spectra of all graphene samples (Figure 2b), which is the excitonic resonance of the interband transition in graphene.[31] This peak and the absorption spectra are insensitive to pressure until the diamondization process occurs. After the transition, the absorbance of all the samples in the energy range of 0.2−1.0 eV (Figure S4) and 1.4−2.5 eV (Figure 2b) drops suddenly and approaches zero gradually with further compression. A weak absorption edge at approximately 2.8 eV is observed in all of the few-layer graphene samples, followed by continuous increases of absorption at higher photon energy. The diamondization pressures are ∼28.3, ∼20.6, and ∼19.4 GPa for tri-, hexa-, and 12-layer graphene, as demonstrated in Figure 2c, consistent with the electrical transport results. Graphite shows the same transition at ∼16.2 GPa. The optical microscopy observations confirm that tri- and thicker graphene becomes increasingly transparent above the transition pressure (Figure 2a and Figure S5). Under decompression, the high-pressure phase could be preserved to ∼1.0 GPa (Figure S6).

The electrical transport and optical absorption measurements have demonstrated that mechanically exfoliated graphene with layer thickness ranging from tri-, tetra-, hexa-, 12- to multilayer undergoes a systematic sp^2−sp^3 diamondization transition under compression and the high-pressure phase has a similar electronic structure. Given the weak X-ray diffraction (XRD) signal of a single few-layer graphene sheet, we conducted XRD measurements on mixed few-layer graphene powders (mainly consisted of tri- to 8-layer graphene sheets, Figure S7) to study the structure of the high-pressure phase. To minimize the possible interaction between each graphene sheet, the mixed tri- to 8-layer graphene powders were sonicated in a pressure medium (Daphane 7373 or silicon oil) for several hours before loading into a diamond anvil cell. The low solidification pressure of the pressure medium could mitigate the interaction between graphene sheets under compression. It is still possible that thicker graphene may form due to the interaction of the mixed tri- to 8-layer graphene sheets, but it does not affect the structural identification of the high-pressure phase based on the coherent diamondization transition in trilayer and thicker graphene under compression. The XRD results show that a new broad diffraction peak (marked as a red arrow in Figure 3) centered between the (100) and (101) peaks of mixed tri- to 8-layer graphene powders appears above 28.5 GPa, and its intensity increases with pressure. Above 50.3 GPa, all of the diffraction peaks of the starting graphene powders disappear, and the sample becomes transparent. In other experimental runs with more samples loaded, XRD measurements indicate that while the starting pressure is almost the same, the structural transition does not complete even above 70 GPa. It is found that the larger the sample size is, the higher the pressure required to finish the structural transition is, consistent with previous observations in different thickness of samples.[23] During decompression, the high-pressure phase can be preserved to a few GPa, consistent with previously reported results on graphene nanoplates.[32,33]

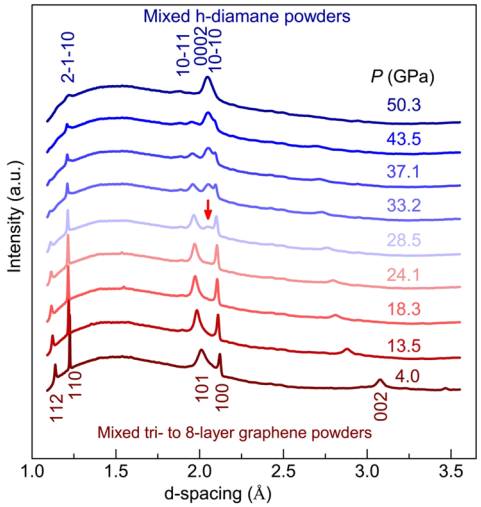

Figure 3. XRD results of mixed tri- to 8-layer graphene powders under compression indicating the structural transition to an atomically thin h-diamondlike structure at 28.5 GPa.

The high-pressure phase of the mixed tri- to 8-layer graphene powders above 50.3 GPa can be indexed with a h-diamondlike structure (Figure S9). The obtained lattice parameters at 50.3 GPa are a = 2.429 ± 0.007 Å and c = 4.095 ± 0.005 Å, respectively. Because h-diamond has a similar bulk modulus as c-diamond, we estimate the unit cell volume of h-diamond under pressure with the equation of state of c-diamond.[34] An ideal a value of ∼2.439 Å is obtained based on the estimated unit cell volume at 50.3 GPa and the ideal c/a = 1.635 of h-diamond.[21,35] Our experimental a value is slightly smaller than the ideal value, which could be partially caused by the structural distortion induced by the nonhydrostatic pressure conditions above 50.3 GPa, as observed in the h-diamond synthesized with compression (c/a = 1.664 at 25 GPa).[26] Furthermore, the broad diffraction peaks above 50.3 GPa also increase the fitting uncertainty during refinements. Other predicted structures, such as H-, R-, W-, and Z-carbon, do not fit the observed XRD pattern.[36−40] The previously reported M-carbon based on XRD results is also not the case of our high-pressure phase.[24] The feature peak of M-carbon at ∼2.7 Å is not observed in our high-pressure phase. We noticed that previous XRD and Raman study on graphene powders observed a structural transition above 18.1 GPa but the local sp^2 hybridization was still maintained.[32] The difference from our results could be caused by the gradual structural transition under compression, as demonstrated in our XRD results (Figure 3). Fifty gigapascals may be not enough to complete the structural transition when a large size of sample is loaded, and thus the sp^2 signal they observed could be from the remaining graphene samples. According to the systematic diamondization transition in compressed trilayer and thicker graphene, and the high-pressure structure of mixed tri- to 8-

https://dx.doi.org/10.1021/acs.nanolett.0c01872
Nano Lett. 2020, 20, 5916−5921

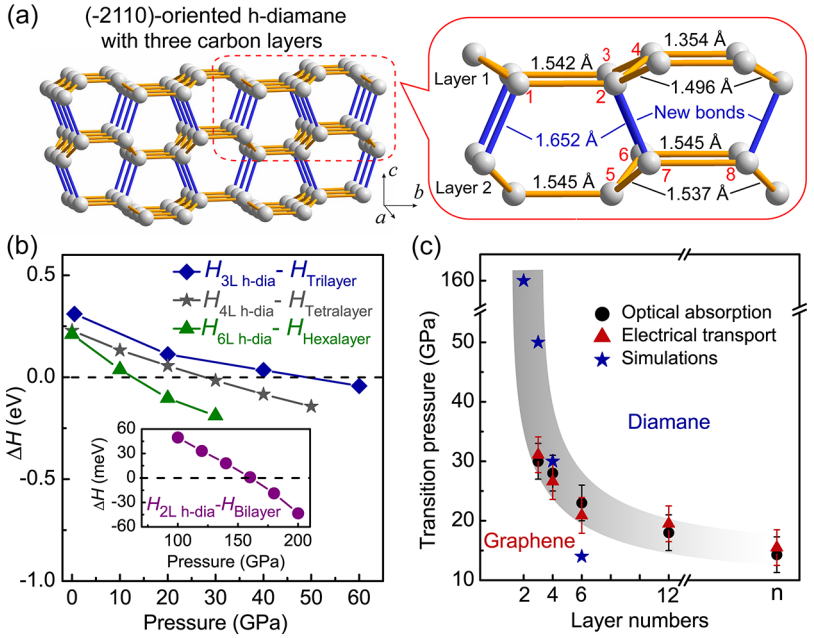

Figure 4. Structure of (−2110)-oriented h-diamane with three carbon layers and the enthalpies of h-diamane (relative to their few-layer graphene precursors) as a function of pressure. (a) Structure of the (−2110)-oriented h-diamane with three carbon layers transformed from trilayer graphene obtained from extensive structure searches. The inset shows the structure details in the dashed red box. The red numbers mark the atoms for plane angle between P_{123} (the plane of the 1, 2, and 3 carbon atoms) and P_{234}, and the plane angle between P_{567} and P_{678}. (b) Enthalpies of (−2110)-oriented h-diamane with two, three, four, and six carbon layers (abbreviated as 2L, 3L, 4L, and 6L h-dia.) as a function of pressure (relative to bi-, tri-, tetra-, and hexa-layer graphene). (c) The layer number dependence of the graphene-diamane transition pressure.

layer graphene powders, it is reasonable to infer that the high-pressure phase of tri-, tetra-. hexa-, and 12-layer graphene also has a structure similar to atomically thin h-diamond, that is, h-diamane. The transition mechanism from few-layer graphene to h-diamane may be associated with a pressure-driven interlayer sliding between adjacent carbon layers, similar to the transition path from hexagonal graphite to h-diamond.[41] Pressure-induced interlayer sliding has also been observed in other atomically thin film samples.[42]

The XRD measurements have shown that the few-layer graphene to h-diamane transition is a gradual structural transition, which helps to understand the continuous resistance increase and absorbance decrease in trilayer and thicker graphene with pressure above the transition pressure. After the structural transition occurs, the sheet resistance is dominated by the few-layer graphene/h-diamane mixture phase. The ratio of h-diamane is low at the onset transition pressure and has little contribution to the physical properties of the mixture phase, therefore, the sheet resistance and absorbance show a continuous transition rather than a sharp jump. With further compression, an increasing fraction of h-diamane causes the sheet resistance to increase, eventually going beyond the measurable range of the instrument, and the absorbance to decrease, gradually approaching zero below the absorption edge.

To rationalize the pressure-induced structural evolution of few-layer graphene, we performed extensive structure searches through CALYPSO software, which can predict the energetically stable structure of materials at a given chemical composition and external conditions, for example, pressure.[43] The extensive structure searches using trilayer graphene as the starting material show that a (−2110)-oriented h-diamane with three carbon layers, as shown in Figure 4a, is energetically stable and has a lower free energy than trilayer graphene precursor above 50 GPa (Figure 4b and Figure S11). In this structure, all of the inner carbons and parts of the surface carbons are sp^3 hybridized, and the remaining surface carbons show sp^2 coupling with bond lengths of 1.354 Å. The angle between P_{123} (Figure 4a) and P_{234} is about 143°, much larger than that of P_{567} and P_{678} (128°), which makes the surface carbon layers relatively flat compared to the inner carbon layers. All of these features contribute to the stability of (−2110)-oriented h-diamane even without hydrogenation or fluorination on the surface. The same transitions are also observed at lower onset pressures for thicker graphene, for example, 30 and 15 GPa for (−2110)-oriented h-diamane four and six carbon layers, respectively. In bilayer graphene, the (−2110)-oriented h-diamane with two carbon layers does not have a lower energy than bilayer graphene until above 160 GPa (Figure 4b). The layer dependence of the transition pressure shows a good agreement with our electrical and absorption results. Band structure calculations indicate that (−2110)-oriented h-diamane with three, four, and six carbon layers has an indirect energy gap of 2.7−2.9 eV (Figure S12), comparable with the optical absorption values. The calculated bandgap shows a weak dependence with the layer thickness (Figure S13), consistent with previous calculation results.[6] Such a weak dependence was not observed in the absorption measurements, which results from the weak absorption of h-diamane that increases the fitting uncertainty of the bandgap.

In summary, pristine h-diamane with three or more carbon layers has been successfully synthesized by diamondization of a mechanically exfoliated trilayer and thicker graphene via compression; once synthesized, it can be preserved upon decompression to ~1.0 GPa. The transition pressure depends greatly on the number of graphene layers, that is, a higher pressure in thinner samples. Optical absorption and band structure calculations reveal that h-diamane has an indirect

https://dx.doi.org/10.1021/acs.nanolett.0c01872
Nano Lett. 2020, 20, 5916−5921

energy gap of 2.8 ± 0.3 eV. Thermal treatment at high pressure may be helpful to preserve a pristine h-diamane to ambient pressure, as suggested from the high-temperature and high-pressure method to synthesize a pressure quenchable h-diamond. Like the discovery of graphene, carbon nanotubes, fullerenes, and other novel carbon allotropes, the realization of a pristine diamane represents another exciting achievement in materials science. Compared to gapless graphene, semiconducting h-diamane could enable new potential applications using carbon-based electronic devices.

■ ASSOCIATED CONTENT

Supporting Information

The Supporting Information is available free of charge at https://pubs.acs.org/doi/10.1021/acs.nanolett.0c01872.

Experimental and calculation details; Figures S1−S13 (PDF)

■ AUTHOR INFORMATION

Corresponding Authors

Bin Chen − *Center for High Pressure Science and Technology Advanced Research, Shanghai 201203, China;* Email: chenbin@hpstar.ac.cn

Feng Ke − *Center for High Pressure Science and Technology Advanced Research, Shanghai 201203, China; Department of Geological Sciences, Stanford University, Stanford, California 94305, United States; Stanford Institute for Materials and Energy Sciences, SLAC National Accelerator Laboratory, Menlo Park, California 94025, United States;* orcid.org/0000-0002-1906-9636; Email: feng17@stanford.edu

Authors

Lingkong Zhang − *Center for High Pressure Science and Technology Advanced Research, Shanghai 201203, China*

Yabin Chen − *Department of Materials Science and Engineering, University of California, Berkeley, California 94720, United States; School of Aerospace Engineering, Beijing Institute of Technology, Beijing 100081, China;* orcid.org/0000-0002-5180-2009

Ketao Yin − *Department of Physics and Engineering Physics, University of Saskatchewan, Saskatoon, Saskatchewan S7N 5E2, Canada;* orcid.org/0000-0002-6179-3409

Chenxu Wang − *Department of Geological Sciences, Stanford University, Stanford, California 94305, United States*

Yan-Kai Tzeng − *Department of Physics, Stanford University, Stanford, California 94305, United States;* orcid.org/0000-0003-3603-1661

Yu Lin − *Stanford Institute for Materials and Energy Sciences, SLAC National Accelerator Laboratory, Menlo Park, California 94025, United States;* orcid.org/0000-0001-5174-9546

Hongliang Dong − *Center for High Pressure Science and Technology Advanced Research, Shanghai 201203, China*

Zhenxian Liu − *Department of Physics, University of Illinois at Chicago, Chicago, Illinois 60607, United States*

John S. Tse − *Department of Physics and Engineering Physics, University of Saskatchewan, Saskatoon, Saskatchewan S7N 5E2, Canada;* orcid.org/0000-0001-8389-7615

Wendy L. Mao − *Department of Geological Sciences, Stanford University, Stanford, California 94305, United States; Stanford Institute for Materials and Energy Sciences, SLAC National Accelerator Laboratory, Menlo Park, California 94025, United States*

Junqiao Wu − *Department of Materials Science and Engineering, University of California, Berkeley, California 94720, United States;* orcid.org/0000-0002-1498-0148

Complete contact information is available at: https://pubs.acs.org/10.1021/acs.nanolett.0c01872

Author Contributions

F.K., L.Z., and Y.C. contributed equally to this work.

Notes

The authors declare no competing financial interest.

■ ACKNOWLEDGMENTS

We thank Drs. Hongwei Sheng, Xiao-Jia Chen, and Lin Wang for their helpful discussions and technical support. The device fabrication done in Berkeley was supported by the U.S. NSF Grant DMR-1708448. Atomic force microscope measurements and data analysis are supported by Mr. Zhe Dong. The authors acknowledge the support of National Natural Science Foundation of China (Grants 51527801 and U1530402). Contribution by Y.L., W.L.M., and F. K. to the experiments, data analysis, and manuscript revising were supported by the U.S. Department of Energy, Office of Science, Basic Energy Sciences, Materials Sciences and Engineering Division (DE-AC02-76SF00515). We thank the beamline scientist of Beamline 12.2.2 at the Advanced Light Source. Beamline 12.2.2 is a DOE Office of Science User Facility under contract no. DE-AC02-05CH11231.

■ REFERENCES

(1) Novoselov, K. S.; Geim, A. K.; Morozov, S. V.; Jiang, D.; Zhang, Y.; Dubonos, S. V.; Grigorieva, I. V.; Firsov, A. A. Electric field effect in atomically thin carbon films. *Science* **2004**, *306*, 666−669.

(2) Zhang, Y.; Tan, Y.-W.; Stormer, H. L.; Kim, P. Experimental observation of the quantum Hall effect and Berry's phase in graphene. *Nature* **2005**, *438*, 201−204.

(3) Novoselov, K. S.; Jiang, Z.; Zhang, Y.; Morozov, S.; Stormer, H. L.; Zeitler, U.; Maan, J.; Boebinger, G.; Kim, P.; Geim, A. K. Room-temperature quantum Hall effect in graphene. *Science* **2007**, *315*, 1379−1379.

(4) McCann, E.; Fal'ko, V. I. Landau-level degeneracy and quantum Hall effect in a graphite bilayer. *Phys. Rev. Lett.* **2006**, *96*, No. 086805.

(5) Cao, Y.; Fatemi, V.; Fang, S.; Watanabe, K.; Taniguchi, T.; Kaxiras, E.; Jarillo-Herrero, P. Unconventional superconductivity in magic-angle graphene superlattices. *Nature* **2018**, *556*, 43−50.

(6) Kvashnin, A. G.; Sorokin, P. B. Lonsdaleite films with nanometer thickness. *J. Phys. Chem. Lett.* **2014**, *5*, 541−548.

(7) Chernozatonskii, L. A.; Sorokin, P. B.; Kvashnin, A. G. e.; Kvashnin, D. G. e. Diamond-like C_2H nanolayer, diamane: Simulation of the structure and properties. *JETP Lett.* **2009**, *90*, 134−138.

(8) Chernozatonskii, L. A.; Sorokin, P. B.; Kuzubov, A. A.; Sorokin, B. P.; Kvashnin, A. G.; Kvashnin, D. G.; Avramov, P. V.; Yakobson, B. I. Influence of size effect on the electronic and elastic properties of diamond films with nanometer thickness. *J. Phys. Chem. C* **2011**, *115*, 132−136.

(9) Jiang, S.; Arguilla, M. Q.; Cultrara, N. D.; Goldberger, J. E. Covalently-controlled properties by design in group IV graphane analogues. *Acc. Chem. Res.* **2015**, *48*, 144−151.

(10) Bakharev, P. V.; Huang, M.; Saxena, M.; Lee, S. W.; Joo, S. H.; Park, S. O; Dong, J.; Camacho-Mojica, D. C.; Jin, S.; Kwon, Y.; Biswal, M.; Ding, F.; Kwak, S. K.; Lee, Z.; Ruoff, R. S. Chemically induced transformation of chemical vapour deposition grown bilayer graphene into fluorinated single-layer diamond. *Nat. Nanotechnol.* **2020**, *15*, 59−66.

(11) Barboza, A. P. M.; Guimaraes, M. H. D.; Massote, D. V. P.; Campos, L. C.; Barbosa Neto, N. M.; Cancado, L. G.; Lacerda, R. G.;

Chacham, H.; Mazzoni, M. S. C.; Neves, B. R. A. Room-Temperature Compression-Induced Diamondization of Few-Layer Graphene. *Adv. Mater.* **2011**, *23*, 3014−3017.
(12) Martins, L. G. P.; Matos, M. J. S.; Paschoal, A. R.; Freire, P. T. C.; Andrade, N. F.; Aguiar, A. L.; Kong, J.; Neves, B. R. A.; de Oliveira, A. B.; Mazzoni, M. S. C.; Filho, A. G. S.; Cancado, L. G. Raman evidence for pressure-induced formation of diamondene. *Nat. Commun.* **2017**, *8*, 96.
(13) Gao, Y.; Cao, T.; Cellini, F.; Berger, C.; de Heer, W. A.; Tosatti, E.; Riedo, E.; Bongiorno, A. Ultrahard carbon film from epitaxial two-layer graphene. *Nat. Nanotechnol.* **2018**, *13*, 133−138.
(14) Antipina, L. Y.; Sorokin, P. B. Converting chemically functionalized few-layer graphene to diamond films: a computational study. *J. Phys. Chem. C* **2015**, *119*, 2828−2836.
(15) Kvashnin, A. G.; Chernozatonskii, L. A.; Yakobson, B. I.; Sorokin, P. B. Phase diagram of quasi-two-dimensional carbon, from graphene to diamond. *Nano Lett.* **2014**, *14*, 676−681.
(16) Leenaerts, O.; Partoens, B.; Peeters, F. Hydrogenation of bilayer graphene and the formation of bilayer graphane from first principles. *Phys. Rev. B: Condens. Matter Mater. Phys.* **2009**, *80*, 245422.
(17) Odkhuu, D.; Shin, D.; Ruoff, R. S.; Park, N. Conversion of multilayer graphene into continuous ultrathin sp^3-bonded carbon films on metal surfaces. *Sci. Rep.* **2013**, *3*, 3276.
(18) Nicolle, J.; Machon, D.; Poncharal, P.; Pierre-Louis, O.; San-Miguel, A. Pressure-mediated doping in graphene. *Nano Lett.* **2011**, *11*, 3564−3568.
(19) Proctor, J. E.; Gregoryanz, E.; Novoselov, K. S.; Lotya, M.; Coleman, J. N.; Halsall, M. P. High-pressure Raman spectroscopy of graphene. *Phys. Rev. B: Condens. Matter Mater. Phys.* **2009**, *80*, No. 073408.
(20) Machon, D.; Bousige, C.; Alencar, R.; Torres-Dias, A.; Balima, F.; Nicolle, J.; de Sousa Pinheiro, G.; Souza Filho, A. G.; San-Miguel, A. Raman scattering studies of graphene under high pressure. *J. Raman Spectrosc.* **2018**, *49*, 121−129.
(21) Bundy, F. P.; Kasper, J. S. Hexagonal diamond-a new form of carbon. *J. Chem. Phys.* **1967**, *46*, 3437−3446.
(22) Aust, R. B.; Drickamer, H. G. Carbon: A new crystalline phase. *Science* **1963**, *140*, 817−819.
(23) Utsumi, W.; Yagi, T. Light-transparent phase formed by room-temperature compression of graphite. *Science* **1991**, *252*, 1542−1544.
(24) Wang, Y.; Panzik, J. E.; Kiefer, B.; Lee, K. K. M. Crystal structure of graphite under room-temperature compression and decompression. *Sci. Rep.* **2012**, *2*, 520.
(25) Patterson, J. R.; Kudryavtsev, A.; Vohra, Y. K. X-ray diffraction and nanoindentation studies of nanocrystalline graphite at high pressures. *Appl. Phys. Lett.* **2002**, *81*, 2073−2075.
(26) Yagi, T.; Utsumi, W.; Yamakata, M.-a.; Kikegawa, T.; Shimomura, O. High-pressure in situ x-ray-diffraction study of the phase transformation from graphite to hexagonal diamond at room temperature. *Phys. Rev. B: Condens. Matter Mater. Phys.* **1992**, *46*, 6031.
(27) Mao, W. L.; Mao, H.-k.; Eng, P. J.; Trainor, T. P.; Newville, M.; Kao, C.-c.; Heinz, D. L.; Shu, J.; Meng, Y.; Hemley, R. J. Bonding changes in compressed superhard graphite. *Science* **2003**, *302*, 425−427.
(28) Hanfland, M.; Syassen, K.; Sonnenschein, R. Optical reflectivity of graphite under pressure. *Phys. Rev. B: Condens. Matter Mater. Phys.* **1989**, *40*, 1951.
(29) Zhao, Y. X.; Spain, I. L. X-ray diffraction data for graphite to 20 GPa. *Phys. Rev. B: Condens. Matter Mater. Phys.* **1989**, *40*, 993.
(30) Goncharov, A. F.; Makarenko, I. N.; Stishov, S. M. Graphite at pressures up to 55 GPa: Optical properties and raman spectra. *High Pressure Res.* **1990**, *4*, 345−347.
(31) Mak, K. F.; Shan, J.; Heinz, T. F. Seeing many-body effects in single-and few-layer graphene: observation of two-dimensional saddle-point excitons. *Phys. Rev. Lett.* **2011**, *106*, No. 046401.
(32) Clark, S. M.; Jeon, K.-J.; Chen, J.-Y.; Yoo, C.-S. Few-layer graphene under high pressure: Raman and X-ray diffraction studies. *Solid State Commun.* **2013**, *154*, 15−18.
(33) Lu, S.; Yao, M.; Yang, X.; Li, Q.; Xiao, J.; Yao, Z.; Jiang, L.; Liu, R.; Liu, B.; Chen, S.; et al. High pressure transformation of graphene nanoplates: a Raman study. *Chem. Phys. Lett.* **2013**, *585*, 101−106.
(34) Occelli, F.; Loubeyre, P.; LeToullec, R. Properties of diamond under hydrostatic pressures up to 140 GPa. *Nat. Mater.* **2003**, *2*, 151−154.
(35) Turneaure, S. J.; Sharma, S. M.; Volz, T. J.; Winey, J.; Gupta, Y. M. Transformation of shock-compressed graphite to hexagonal diamond in nanoseconds. *Sci. Adv.* **2017**, *3*, No. eaao3561.
(36) Li, Q.; Ma, Y.; Oganov, A. R.; Wang, H.; Wang, H.; Xu, Y.; Cui, T.; Mao, H.-K.; Zou, G. Superhard monoclinic polymorph of carbon. *Phys. Rev. Lett.* **2009**, *102*, 175506.
(37) He, C.; Sun, L.; Zhang, C.; Peng, X.; Zhang, K.; Zhong, J. New superhard carbon phases between graphite and diamond. *Solid State Commun.* **2012**, *152*, 1560−1563.
(38) Niu, H.; Chen, X.-Q.; Wang, S.; Li, D.; Mao, W. L.; Li, Y. Families of superhard crystalline carbon allotropes constructed via cold compression of graphite and nanotubes. *Phys. Rev. Lett.* **2012**, *108*, 135501.
(39) Wang, J.-T.; Chen, C.; Kawazoe, Y. Low-Temperature Phase Transformation from Graphite to sp^3 Orthorhombic Carbon. *Phys. Rev. Lett.* **2011**, *106*, No. 075501.
(40) Amsler, M.; Flores-Livas, J. A.; Lehtovaara, L.; Balima, F.; Ghasemi, S. A.; Machon, D.; Pailhes, S.; Willand, A.; Caliste, D.; Botti, S.; Miguel, A. S.; Goedecker, S.; Marques, M. A. L. Crystal structure of cold compressed graphite. *Phys. Rev. Lett.* **2012**, *108*, No. 065501.
(41) Khaliullin, R. Z.; Eshet, H.; Kühne, T. D.; Behler, J.; Parrinello, M. Nucleation mechanism for the direct graphite-to-diamond phase transition. *Nat. Mater.* **2011**, *10*, 693−697.
(42) Li, T.; Jiang, S.; Sivadas, N.; Wang, Z.; Xu, Y.; Weber, D.; Goldberger, J. E.; Watanabe, K.; Taniguchi, T.; Fennie, C. J.; Fai Mak, K.; Shan, J. Pressure-controlled interlayer magnetism in atomically thin CrI_3. *Nat. Mater.* **2019**, *18*, 1303−1308.
(43) Wang, Y.; Lv, J.; Zhu, L.; Ma, Y. CALYPSO: A method for crystal structure prediction. *Comput. Phys. Commun.* **2012**, *183*, 2063−2070.

https://dx.doi.org/10.1021/acs.nanolett.0c01872
Nano Lett. 2020, 20, 5916−5921